Analysis of Bifurcated Superstructure of Nonlinear Ocean System

By O. Gottlieb,[1] S. C. S. Yim,[2] Member, ASCE, and H. Lin[3]

Abstract: An intricate universal superstructure in bifurcation sets and routes to chaos of a nonlinear moored ocean system subjected to monochromatic wave excitations are investigated analytically and demonstrated numerically in detail herein. System nonlinearities include complex geometric restoring force and coupled fluid-system exciting forces. Primary and secondary resonance regions are identified by employing variational analysis techniques for local stability. Tangent and periodic doubling bifurcations are examined to reveal the underlying intricate superstructure. Numerical results of this complex system uncover a steady-state superstructure in the bifurcation sets that exhibit a similar bifurcation pattern of coexisting solutions in the subharmonic, ultraharmonic, and ultrasubharmonic domains. Within this superstructure it is illustrated that strange attractors appear when a period doubling sequence is infinite, and when abrupt changes in the size of an attractor occur near tangent bifurcations.

INTRODUCTION

Highly nonlinear (including chaotic) responses have recently been observed in various numerical and approximate semianalytical models of compliant ocean systems (e.g., Bernitsas and Chung 1990; Gottlieb and Yim 1992). (To avoid confusion the word "system" is used exclusively to refer to the physical structural assembly considered. The word "structure" refers to the organization of the bifurcation sets and routes to chaos, which is the focus of this study.) Nonlinearities of these models include restoring force (induced by geometry or discontinuity) and coupled hydrodynamic effects introduced by quadratic fluid-system interaction viscous drag. The inertial component may include a bias external excitation that for certain structural configurations is complemented by an additional coupled nonlinear convective excitation. Moreover, complex and sensitive transverse dynamical responses in low-tensioned, small-sag, inelastic (hysteretic) mooring cables have been identified and observed (Triantafyllou and Yue 1995). The system response behavior may become further complicated when the effects of the nonlinear structure-cable interaction become significant.

Numerical investigations of simple systems that exhibit similar nonlinear properties have revealed intricate behavior including coexisting periodic (harmonic, subharmonic, ultraharmonic, and ultrasubharmonic) and aperiodic (quasiperiodic and chaotic) solutions defined by initial conditions. Stability of each type of system responses is governed by complicated phenomena near resonance and sensitivity to initial conditions. The behavior of nonlinear dissipative dynamical systems subjected to deterministic excitation has been studied extensively by both classical and modern techniques. Classical techniques have concentrated on obtaining closed form periodic solutions of integrable or weakly nonlinear systems and analyzing their stability (Nayfeh and Mook 1979). Modern techniques concentrate on global bifurcations and address the existence of chaotic responses and global system behavior (Guckenheimer and Holmes 1986).

It is well known that chaotic behavior is inherent in a general class of nonlinear systems (e.g., Thompson and Stewart 1986). Its existence can be identified by the application of modern quantitative measures. Examples of such measures are Lyapunov exponents, and fractal or multifractal dimensions.

A less-recognized aspect of the global nonlinear behavior of these systems is the existence of an elaborate "superstructure," including crisis and intermittent phenomena (Grebogi et al. 1983) that organizes the bifurcation sets (Ueda et al. 1990). The presence of a superstructure in the bifurcation sets of a nonlinear system enables a comprehensive overview of its global behavior. Although no methodology has been developed at this point, the precise nature of the superstructure and its sensitivity to small changes in numerical values of system parameters may potentially be employed in the future to provide an excellent tool for identification of highly nonlinear systems when experimental measurements are available.

While a large number of dynamical systems exhibit at first glance a nonlinear structure similar to that of one-dimensional (1D) maps (e.g., Simoyi et al. 1982), detailed numerical analysis of continuous dynamical systems reveals that at least a codimension two bifurcation analysis is needed to adequately describe a nonlinear system behavior. Parlitz and Lauterborn (1985) demonstrated numerically the existence of a superstructure in the bifurcation sets of a system with simple nonlinearity idealized by a Duffing equation with a single-well potential. They related their findings to ultraharmonic and ultrasubharmonic resonant properties of the system and conjectured that the superstructure is universal to a large class of nonlinear oscillators with simple or complex nonlinearities.

Recently Ueda et al. (1990) demonstrated the global bifurcation organizing behavior of another simple system represented by a Duffing equation with a double-well potential. Grebogi et al. (1987) and Thompson and Soliman (1990) numerically investigated fractal basin boundary bifurcations and determined the corresponding generic codimension-two patterns. They also conjectured the behavior to be universal in all forced dissipative systems.

Motivated by the potential practical applications of the superstructure to analyze the global behavior and to identify parameters of highly nonlinear systems, the present study numerically examines in detail the underlying patterns of the nonlinear motions of the moored ocean system with complex stiffness and forcing nonlinearities considered by Gottlieb and Yim (1992). We first summarize a local stability analysis for the development of bifurcation criteria of the various nonlinear responses, including resonance, subharmonic, ultraharmonic, ultrasubharmonic, and chaotic motions. Guided by the stability regions delineated by the bifurcation criteria, the existence of the periodic recurrence of a superstructure in the bifurcation sets is then demonstrated by carefully examining the numerical

[1]Facu. of Mech. Engrg., Technion–Israel Inst. of Tech., Haifa, Israel.
[2]Prof., Dept. of Civ. Engrg., Oregon State Univ., Corvallis, OR 97331.
[3]Res. Assoc., Dept. of Civ. Engrg., Oregon State Univ., Corvallis, OR.

Note. Associate Editor: Sami F. Masri. Discussion open until April 1, 1998. To extend the closing date one month, a written request must be filed with the ASCE Manager of Journals. The manuscript for this paper was submitted for review and possible publication on April 12, 1996. This paper is part of the ***Journal of Engineering Mechanics***, Vol. 123, No. 11, November, 1997. ©ASCE, ISSN 0733-9399/97/0011-1180–1187/$4.00 + $.50 per page. Paper No. 13054.

results documented in Gottlieb and Yim (1992) and additional ones presented here. The superstructure underlying the bifurcation sets illustrates an intricate universal bifurcation pattern of coexisting solutions in the subharmonic, ultraharmonic, and ultrasubharmonic domains. Within this superstructure strange attractors appear when a period doubling bifurcation sequence is infinite (Feigenbaum 1980) and when an abrupt change in the size of a unique attractor (Ueda 1981) occurs near a tangent bifurcation value. The superstructure is closely related to the nonlinear resonances of the system and enables identification of routes to chaos and their relationship with other instabilities for given environmental conditions.

SYSTEM CONSIDERED

A submerged, neutrally buoyant multipoint moored ocean system shown in Fig. 1 is modeled as a single degree of freedom (SDOF, $x_3 = x_5 = 0$) rigid body in surge, hydrodynamically damped, and excited nonlinear oscillator. The equation of motion is derived based on equilibrium of geometric restoring forces and dynamic forces induced by body motion under monochromatic wave and uniform current excitation. The governing equation is given by (Gottlieb and Yim 1992)

$$(M + \rho \forall C_A)\ddot{x}_1 + C\dot{x}_1 + 4K\left\{x_1 - \frac{l_c}{2d}\left[\frac{\beta + x_1}{\sqrt{1 + (\beta + x_1)^2}} - \frac{\beta - x_1}{\sqrt{1 + (\beta - x_1)^2}}\right]\right\} = F_D + F_I = \frac{\rho}{2} C_D A_P (u_1 - \dot{x}_1)|u_1 - \dot{x}_1| + \rho \forall (1 + C_A)\left[\frac{\partial u_1}{\partial t} + (u_1 - \dot{x}_1)\frac{\partial u_1}{\partial x_1}\right] \quad (1a)$$

where M = body mass; C = system damping coefficient; K = elastic coefficient of mooring line; β denotes the degree of geometric nonlinearity; l_c = initial length of mooring lines (see Fig. 1 for d); C_D and C_A = hydrodynamic viscous drag and added mass coefficients, respectively; A_P = projected drag area; $\forall$ = displace volume; ρ = water mass density; x_1 represents the surge displacement; and u_1 = fluid particle velocity. Moreover, u_1 and β are given by

$$u_1 = U_0 + \omega a \frac{\cosh kh}{\sinh kh} \cos(kx_1 - \omega t); \quad \beta = \frac{2b - L}{2d} \quad (1b)$$

where U_0 denotes colinear current magnitude; a, ω, and k = wave amplitude, frequency, and number, respectively; L = diameter of the sphere (see Fig. 1 for b); and h = water depth.

After normalization with respect to the total mass ($M + \rho \forall C_A$) and distance d, and introducing time as an additional variable, (1a) can be rewritten as an autonomous system

$$\dot{x} = y; \quad \dot{y} = -R(x) - \gamma y + F_D(x, y, \theta) + F_I(x, y, \theta); \quad \dot{\theta} = \omega \quad (2a,b,c)$$

where x and y = normalized surge displacement and velocity, respectively; $R(x)$ denotes the normalized restoring force; F_D = normalized drag force; F_I = normalized initial force; and γ = normalized system damping coefficient (see Appendix I for expressions).

As shown in (1) the complex nature of the moored ocean system results from the highly nonlinear relationships between the stiffness, coupled drag, and inertia excitation forces and the (large) displacement and velocity responses. The stiffness nonlinearity is due to the mooring angle (geometry), which can vary from a highly nonlinear two-point system ($b = 0$) to an almost linear four-point system ($b >> d$). The mooring lines considered in this study are assumed to be linear, elastic, and taut [$l_c/2d = \tau = 1/2\sqrt{(1 + \beta^2)}$], and do not vibrate transversely. These simple assumptions are in direct contrast to the nonlinear, inelastic (hysteretic), and low-tensioned cables examined by Triantafyllou and Yue (1995), where the cable properties and sag were the major sources of the nonlinear dynamical phenomena of the system response. Because of the complexity of (1), exact solutions of the response are impractical; approximate solutions need to be developed.

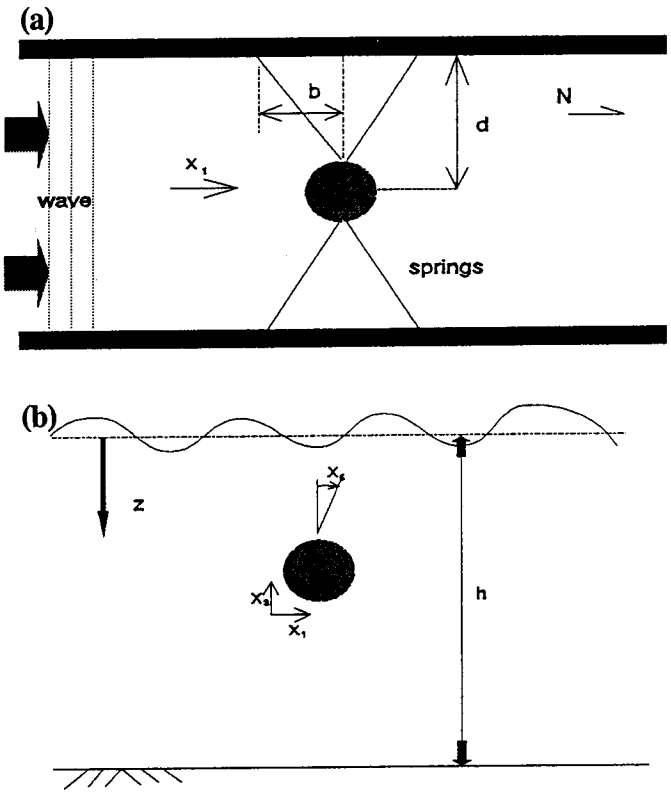

FIG. 1. Multi-Point Moored Ocean System: (a) Plan View; (b) Profile View

APPROXIMATE SOLUTION

As in Gottlieb and Yim (1992), the method of harmonic balance is chosen here for approximate system solutions to account for the even harmonics that are induced by the bias due to the nonlinear viscous drag and convective inertial forces. The following approximate solution form is assumed:

$$x_{0(n/m)} \cong A_{0(n/m)} + \sum_i^I A_{i(n/m)} \cos\left[i\frac{n}{m}\theta + \Psi_{i(n/m)}\right] \quad (3a)$$

$$y_{0(n/m)} \cong -\omega\frac{n}{m}\sum_i^I iA_{i(n/m)} \sin\left[i\frac{n}{m}\theta + \Psi_{i(n/m)}\right] \quad (3b)$$

where $A_{0(n/m)}$, $A_{i(n/m)}$, $\Psi_{i(n/m)}$ = solution amplitudes and phases; I = order of approximation ($i = 1, 2, 3, \ldots, I$); and n/m = order of ultrasubharmonics.

The unknown amplitudes and phases can be derived by substituting the approximate solution [(3)] into the system [(2)], squaring the resulting equation, and comparing terms of equal harmonic order. Thus, the system is transferred into a finite nonlinear set of algebraic equations

$$S_j[A_0, A_{i(n/m)}, \Psi_{i(n/m)}] = 0 \quad (4)$$

where $j = 1, 2, 3, \ldots, 2I + 1$.

Solutions of this set for the unknown amplitudes and phases are obtained by using an iterative Newton-Raphson procedure (Gottlieb and Yim 1992). The frequency response (backbone) curve of the Hamiltonian system, which characterizes the de-

gree of nonlinearity of the system, can then be generated numerically by varying the excitation frequency.

STABILITY ANALYSIS

Local stability of the approximate solution can be determined by considering a perturbed solution, $x(t) = x_0(t) + \varepsilon(t)$, that on substitution in (2) results in a nonlinear variational equation. Linearizing the variational equation yields a set of linear ordinary differential equations with periodic coefficient functions $\{H_{1,2}[x_0(\theta), y_0(\theta)] = H_{1,2}[x_0(\theta + 2\pi), y_0(\theta + 2\pi)]\}$

$$\dot{\varepsilon} = \eta; \quad \dot{\eta} = H_1(x_0, y_0)\eta + H_2(x_0, y_0)\varepsilon \tag{5a}$$

where

$$H_1 = -\gamma - 2\frac{\mu\delta}{\omega}\left|u_0 - \frac{y_0}{\omega}\right| + \mu\omega^2\kappa\left[\frac{1}{\omega} - 1 + \left(u_0 - \frac{y_0}{\omega}\right)\right]u_0 \tag{5b}$$

and

$$H_2 = -\alpha(1 - \tau\{[1 + (\beta + x_0)^2]^{-3/2} + [1 + (\beta - x_0)^2]^{-3/2}\}) - 2\mu\delta\kappa\left|u_0 - \frac{y_0}{\omega}\right|u_0' + \mu\omega^2\kappa^2\left\{(u_0 - f_0)\left[\frac{1}{\kappa} - (u_0 - y_0)\right] + u_0'^2\right\} \tag{5c}$$

In (5*b*) and (5*c*), $u_0 = f_0 + f_1\cos(\kappa x_0 - \theta)$; and α, β, γ, δ, κ, μ, τ, f_0, f_1, and h' are system and excitation parameters (see Appendix I for expressions). Substituting the approximate solution [(3)] into (5*b*) and (5*c*) and expanding $H_{1,2}(x_0, y_0)$ in Fourier series, $[H_{1,2}(\theta)]$, a generalized Hill's variational equation is obtained

$$\dot{\varepsilon} = \eta; \quad \dot{\eta} = H_1(\theta)\eta + H_2(\theta)\varepsilon \tag{6a}$$

where $H_{1,2}$ are given by

$$H_1 = \xi_{0(n/m)} + \sum_j \xi_{Cj(n/m)}\cos\left(j\frac{n}{m}\theta\right) + \xi_{Sj(n/m)}\sin\left(j\frac{n}{m}\theta\right) \tag{6b}$$

and

$$H_2 = \zeta_{0(n/m)} + \sum_j \zeta_{Cj(n/m)}\cos\left(j\frac{n}{m}\theta\right) + \zeta_{Sj(n/m)}\sin\left(j\frac{n}{m}\theta\right) \tag{6c}$$

with (ξ_{Cj}, ζ_{Cj}) and (ξ_{Sj}, ζ_{Sj}) the Fourier coefficients calculated from $H_{1,2}$. The particular solution to (6*a*), $\varepsilon = \exp(\nu t)Z(t)$, with the Floquet theory (Ioos and Joseph 1981) can be used to identify the stability regions for symmetric and unsymmetric responses.

A low order ($I = 1$)2π periodic two-term unsymmetric solution $x_0(\theta) = A_0 + A_1\cos(\theta + \Psi_1)$ corresponding to excitation of small amplitude waves and weak current depicts both tangent and period double bifurcations [Fig. 2(a)]. The primary resonance [originating from (0, 0) in Fig. 2(a)] is obtained by applying harmonic balance method to (6) at the stability limit ($\nu = 0$)

$$\omega^2 = \frac{1}{2}\left\{\alpha\left(\zeta_0 - \frac{\zeta_1^2}{\zeta_0}\right)\gamma^2 \pm \sqrt{\gamma^4 + 2\alpha\gamma^2\left[\left(\frac{\zeta_1}{\zeta_0}\right)^2 - 1\right] + \alpha^2\left[\left(\frac{\zeta_1}{\zeta_0}\right)^2 - \frac{\zeta_2}{\zeta_0}\right]^2}\right\} \tag{7a}$$

where $\zeta_1 = \sqrt{(\zeta_{C1}^2 + \zeta_{S1}^2)}$; and $\zeta_2 = \sqrt{(\zeta_{C2}^2 + \zeta_{S2}^2)}$. The secondary stability region [to the right of the primary resonance in Fig. 2(a)] is obtained by solving (6) inserting the period doubled $\varepsilon(t) = b_{1/2}\cos(\theta)$

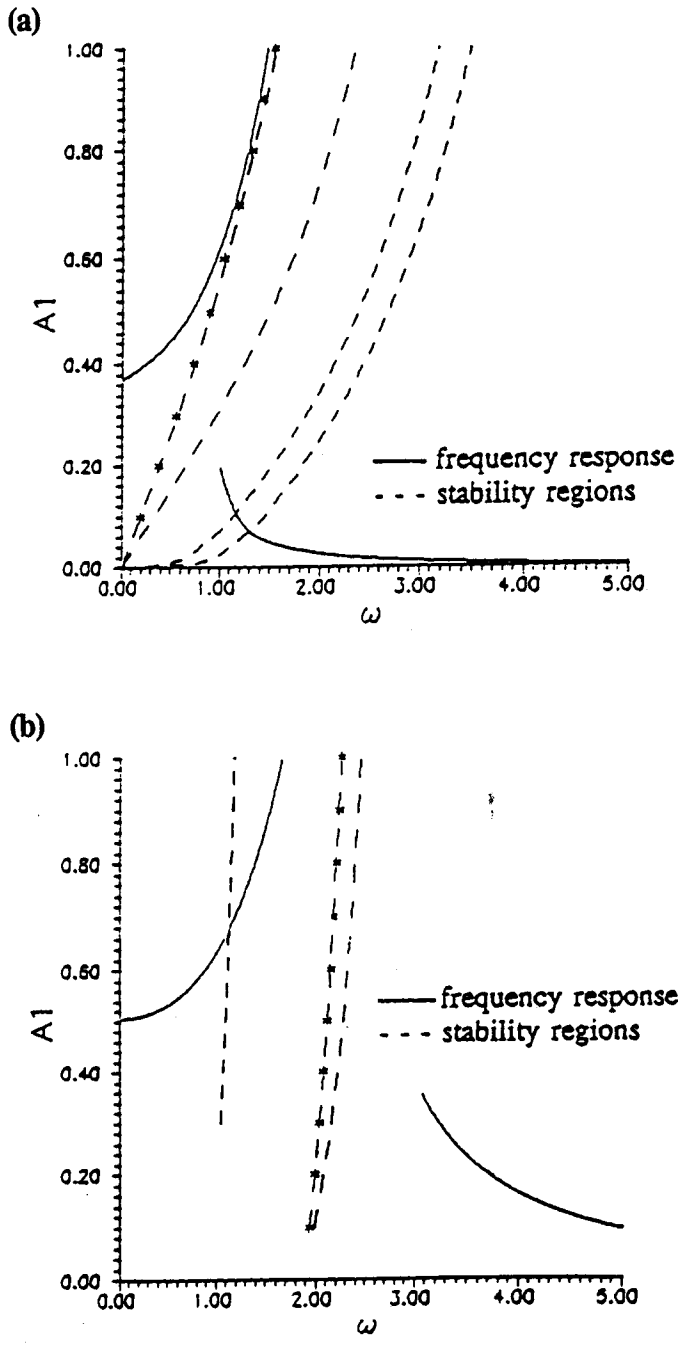

FIG. 2. Stability Diagram of Nonlinear Restoring Force with Linearized Excitation: (a) Wave and Current; (b) Wave

$$\omega^2 = 2(\alpha\zeta_0 - \gamma'^2 \pm \sqrt{\gamma'^4 - 2\alpha\gamma'^2\zeta_0 + \alpha^2\zeta_1^2}) \tag{7b}$$

where $\gamma' = \gamma + (8/3\pi)\mu\delta\sqrt{(f_0^2 + f_1^2)}$.

A low order one-term symmetric solution such as $x_0(\theta) = A_1\cos(\theta + \Psi_1)$, corresponding to the response of small amplitude wave excitation ($f_0 = 0$, $f_1 \neq 0$), does not exhibit a period doubling phenomenon but determines a pitchfork bifurcation in which the $Z(\theta) = Z(\theta + \pi)$ solution loses its stability [Fig. 2(b)]. This approximate order two ultraharmonic stability region boundaries are obtained by solving (6) inserting $\varepsilon(t) = b_0 + b_2\cos(2\theta)$

$$\omega^2 = \frac{1}{8}\left\{\alpha\left(\zeta_0 - \frac{\zeta_2^2}{\zeta_0}\right) - \gamma'^2 \pm \sqrt{\gamma'^4 + 2\alpha\gamma'^2\left[\left(\frac{\zeta_2}{\zeta_0}\right)^2 - 1\right] + \alpha^2\left[\left(\frac{\zeta_2}{\zeta_0}\right)^2 - 2\frac{\zeta_4}{\zeta_0}\right]^2}\right\} \tag{8}$$

Stability loss of both symmetric and unsymmetric solutions

are demonstrated above, and period doubling is indicated (intersections of the frequency curves and stability regions in Fig. 2) and numerically verified. A similar analysis procedure can also apply to identify higher order subharmonic and ultrasubharmonic resonances. Cascades of period doubling bifurcations predicted by the analysis have been numerically confirmed (Gottlieb and Yim 1992).

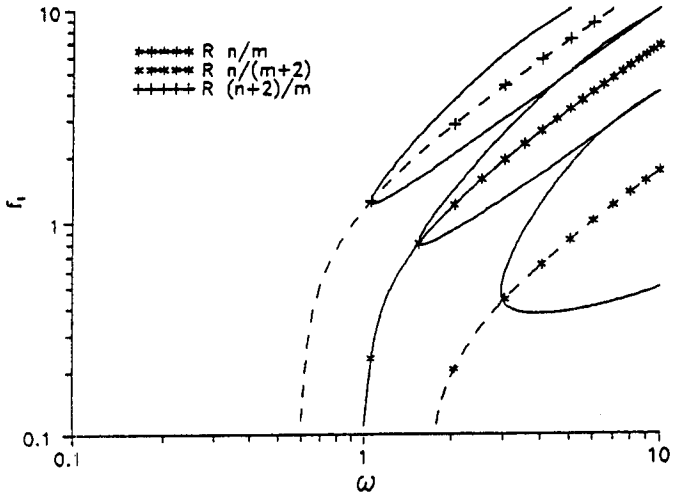

FIG. 3. Superstructure in Bifurcation Sets

TABLE 1. Order of Superstructure in Bifurcation Set

$R_{n/m}$	1	2	3	4		n
1	1/1, 1	2/1, 1	3/1, 1	4/1, 1		$n/1, j$
2	1/2, 1	1/1, 2	3/2, 1	2/1, 2		$n/2, j$
3	1/3, 1	2/3, 1	1/1, 3	4/3, 1		$n/3, j$
4	1/4, 1	1/2, 2	3/4, 1	1/1, 4		$n/4, j$
m	$1/m, j$	$2/m, j$	$3/m, j$	$4/m, j$		$1/1, j$

In the absence of knowledge of the possible existence of an intricate superstructure (see following section), Gottlieb and Yim (1992) conducted a comprehensive numerical study and presented examples of various types of nonlinear responses collaborating the stability regions delineated by (7) and (8). These examples include pitchfork bifurcation, dynamic symmetry breaking, multiple occurrence of unsymmetric subharmonics, period doubling in subharmonic domains, period doubling in ultraharmonic domains, and coexistence of harmonic and multiple subharmonics of different orders (Figs. 7–12, respectively, in Gottlieb and Yim 1992).

IDENTIFICATION OF SUPERSTRUCTURE

As mentioned earlier, the existence of an intricate superstructure in an idealized, simple nonlinear system represented by the Duffing equation with a single-well potential has been shown numerically by Parlitz and Lauterborn (1985). The global behavior shown includes crisis and intermittent phenomena (Grebogi et al. 1983) and organization of the bifurcation sets (Ueda et al. 1990). The superstructure is similar to that observed and analytically determined in codimension-two bifurcation problems in other idealized simple systems such as the Hénon map (Holmes and Whitley 1984) and Circle map (Arnold 1965).

Prompted by these qualitative observations on systems with simple nonlinearities and the numerical results of the system with complex nonlinearities examined by Gottlieb and Yim (1992), a detailed numerical investigation of the superstructure of the moored ocean system is conducted here. The numerical search for the existence of various types of responses and identifying the underlying global pattern is guided by the stability regions in parameter space near low-order (Fig. 2) and higher-order (not shown here) resonances. It is discovered that in the region [$\alpha = 1$, $\beta = (0, 1)$, $\tau = 1/2\sqrt{(1 + \beta^2)}$, $\gamma < \delta = 0.1$, μf, ω] a similar bifurcation pattern for subharmonic, ultraharmonic, and ultrasubharmonic near resonant regions exists. This

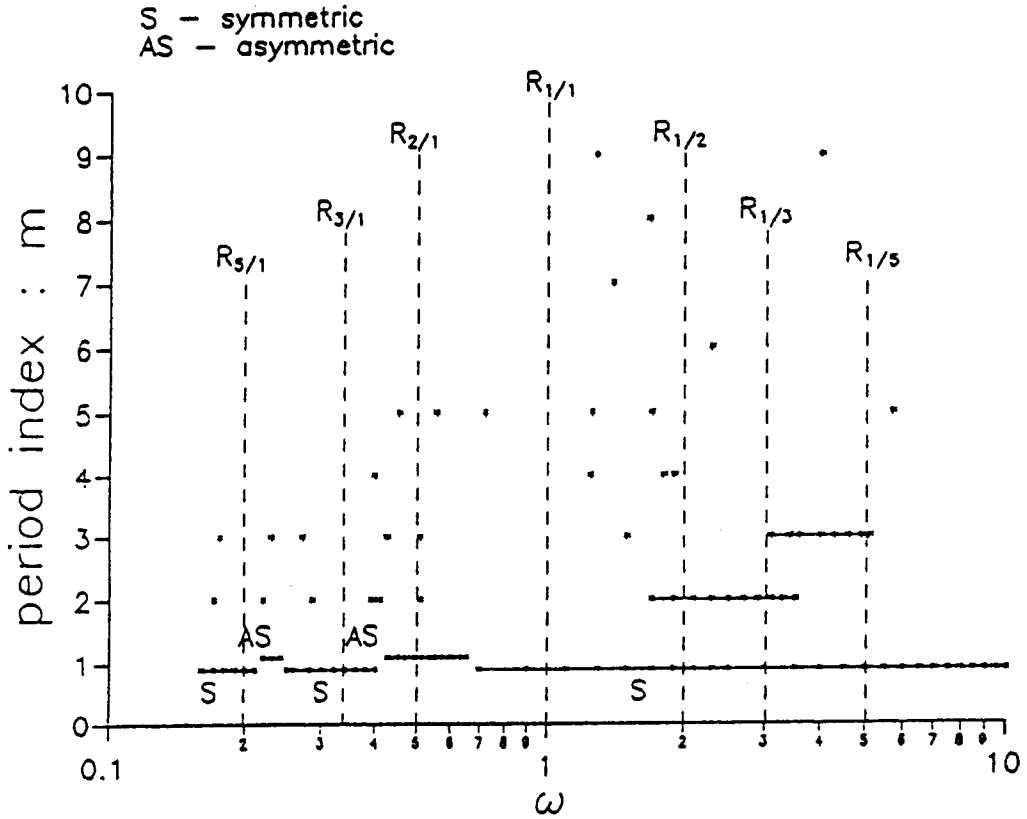

FIG. 4. Bifurcation Diagram

superstructure is presented in Fig. 3. The pattern consists of intersecting "resonance horns" that portray asymptotic behavior for large excitation (μf). Intersecting resonance lines (tangent and homoclinic bifurcations) describing coexisting solutions are also derived for the Hénon map by a number of investigators (e.g., Holmes and Whitley 1984). Note that bifurcations of equivalent periodic families (e.g., $n/m = n/3$) intersect and possess the same slope. The width of the horn is found to be governed by the relative damping ratio ($\gamma^* \propto \gamma/\delta$). Thus a control space defined by parameters describing a nondimensional relationship between excitation and system parameters [μf, ω/ω_0, where $\omega_0 = \omega_0(\alpha, \beta)$, γ/δ] can be derived. Note that the codimension two bifurcations of Ueda (1980) and Ueda et al. (1990) are defined in parameter space by damping versus excitation amplitude whereas Parlitz and Lauterborn (1985) describe their ultraharmonic resonances in terms of excitation amplitude versus frequency.

Classification of the bifurcations defining the superstructure is typically done by a describing bifurcation number. Holmes and Whitley (1984) extend the conventions of 1D maps in their analysis of the 2D Hénon map [i.e., s_m^j where index m is the period determined by Sarkovski's theorem (Devaney 1986) and j is the order of appearance calculated by kneading theory (Guckenheimer and Holmes 1986)]. Ueda et al. (1990) define suffices describing the periodicity (m) and an arbitrary index to distinguish between types of solutions, whereas Parlitz and Lauterborn (1985) define an ultraharmonic index (i.e., number of maximum periodic solutions in one forcing period) complemented by periodicity index to define ultrasubharmonics.

In order to classify the bifurcation pattern of the subharmonic, ultraharmonic, and ultrasubharmonic solutions for the submerged moored system, the nonlinear resonance relationship $n\omega \approx m\sqrt{\alpha_1}$ (where ω = wave excitation frequency; α_1 = coefficient of the linear component of the nonlinear stiffness) is used to determine the first index [n/m] of the resonance number. the ratio n/m (i.e., an inverse 1D winding number), however, can be a relatively prime integer. Consequently, a second index [j], is required to determine the order of ratios

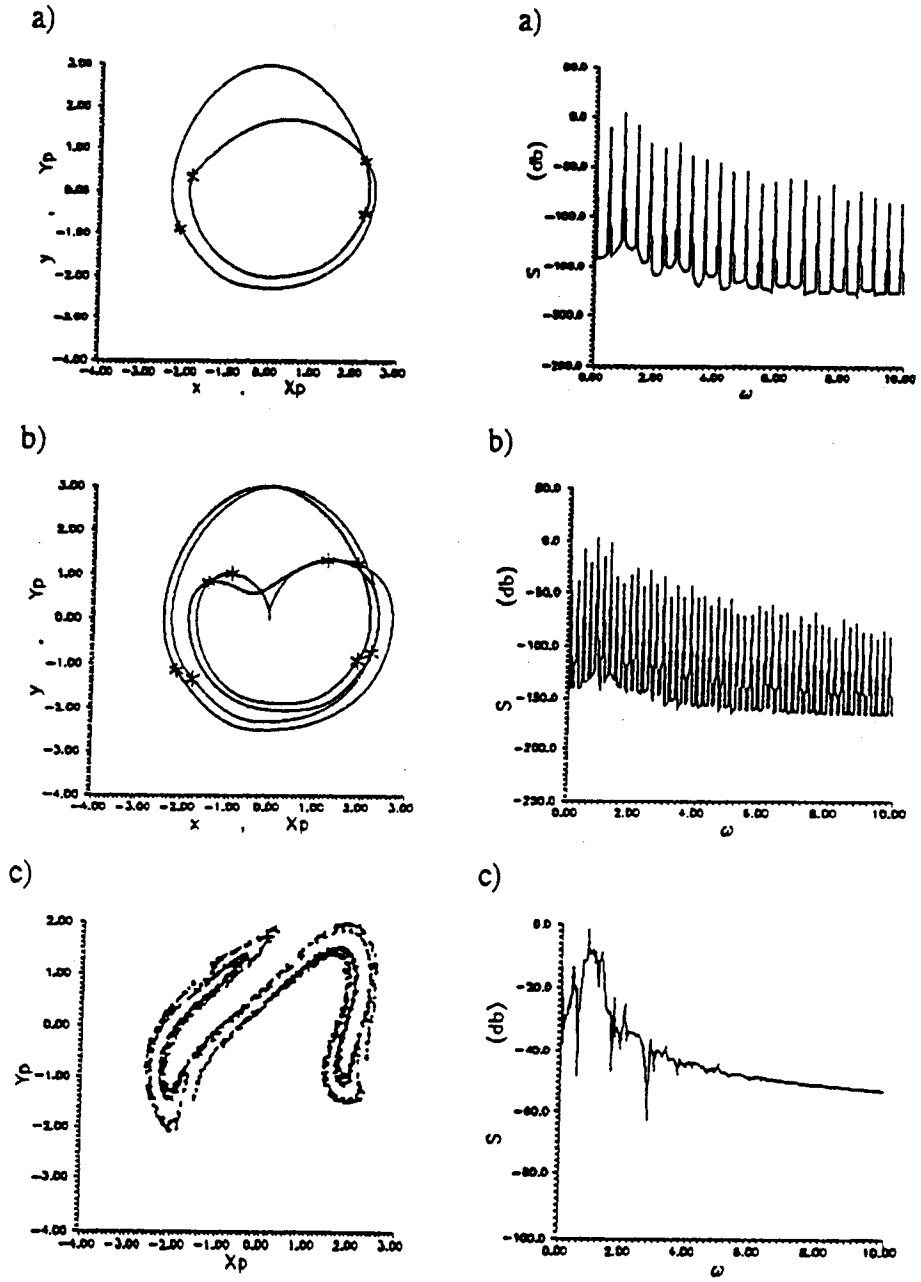

FIG. 5. Evolution of Chaotic Attractor via Period Doubling: (a) $\omega = 1.7$, $(n/m, j) = (1/2, 2)$; (b) $\omega = 1.68$, $(n/m, j) = (1/2, 4)$; (c) $\omega = 1.65$, $(n/m, j) = (\text{"1/2"}, \infty)$

with noncommon factors. Note that m denotes periodicity of the response. Finally, a third index is required to determine the dimension [d] of the response (i.e., integer deterministic versus fractal chaotic). Note that the fractal dimension may not by itself establish the chaotic nature of the motion (e.g., when it is close to an integer value) and a multifractal representation (Feder 1989) is needed to quantify the "strangeness" of systems with two or more degrees of freedom [e.g., the quasiperiodic response of an experimental attractor for thermal convection (Jensen et al. 1985)]. Thus, a resonance number $R_{(n/m,j,d)}$ describing a repeating global bifurcation pattern is defined here.

Table 1 is devised in this study to demonstrate the intricate superstructure in the bifurcation set of the submerged moored system. Knowledge of the intricate superstructure enables identification of coexisting solutions and pitchfork or period doubling bifurcations. The table displays the index of the fundamental resonant structure [n/m] followed by the index of ordering [j]. Note that the upper row and the first column describe the ultra [n] and sub [m] indices, respectively. The index [j] identifies the order of equal ratios [e.g., (n/m, j) = (1/2, 1) at (column, row) = (1, 2) versus (n/m, j) = (1/2, 2) at (column, row) = (2, 4)]. Thus, the table diagonal divides between the ultraharmonic and subharmonic domains. Coexistence found by local analysis can be determined by resonance numbers $R_{(n/m,j)}$ with similar n/m ratios (e.g., $R_{1/2,1}$ and $R_{3/5,1}$). Also note that ultraharmonic solutions described by an even descriptor (n or m) are unsymmetric whereas odd descriptors describe symmetric or self-similar solutions. Numerical examples of coexisting (n/m = 1/2) and (n/m = 4/5) and singly existing self-similar (n/m = 3/5) can be found in Figs. 12 and 9(c) in Gottlieb and Yim (1992), respectively.

The pitchfork bifurcation governed by (8) [shown here in Fig. 2(b)] describes stability loss of a symmetric solution that evolves in parameter space to two partner orbits (see Fig. 8, Gottlieb and Yim 1992). This bifurcation is described by the ordering index j: 1, 2 for n/m = 2/1 (e.g., $R_{2/1,1} \rightarrow R_{2/1,2}$) in the ultraharmonic domain. Similarly, the period doubling bi-

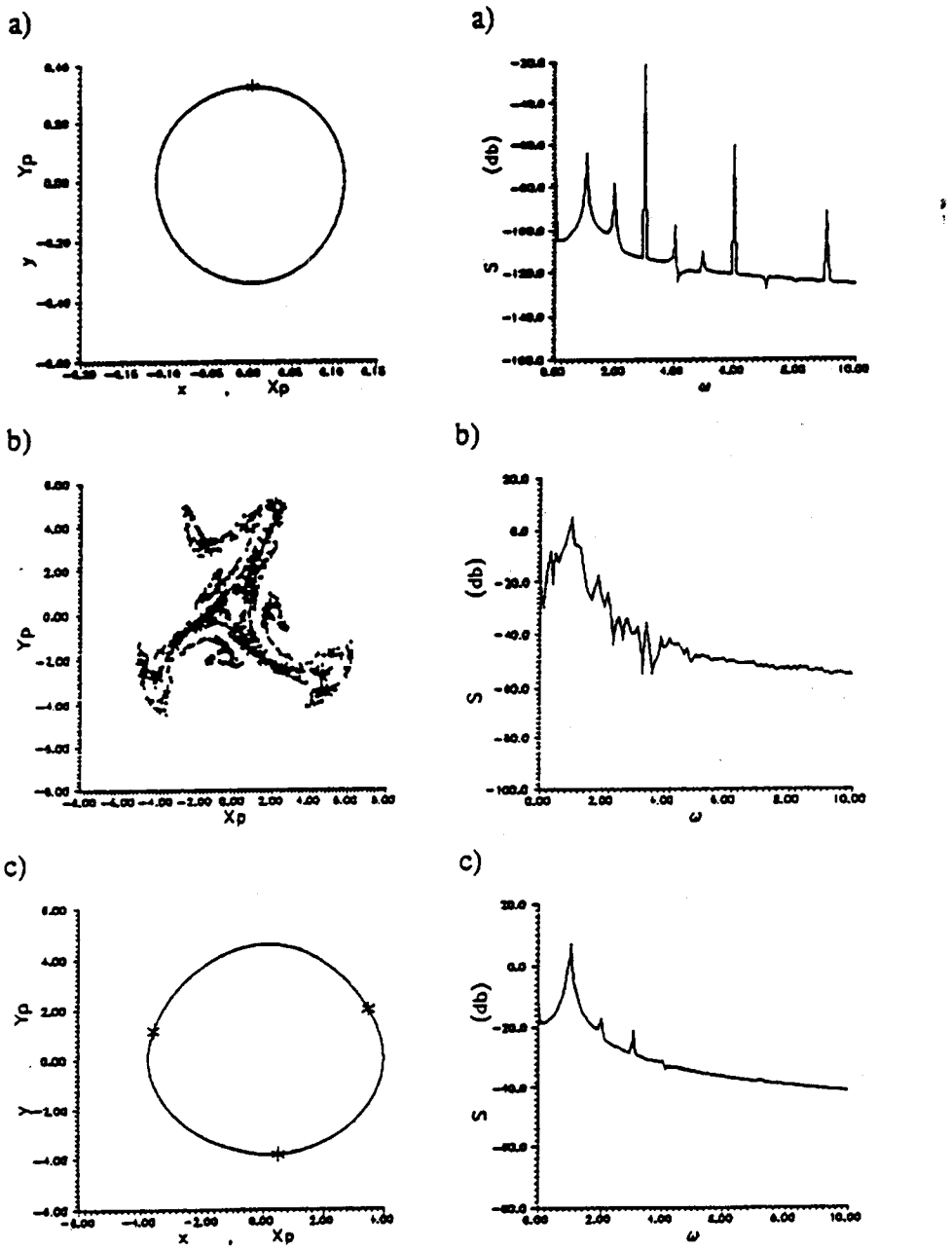

FIG. 6. Evolution of Chaotic Attractor via Explosion: (a) ω = 3.05, (n = m = 1); (b) ω = 3.10, (n/m, j) = ("1/2", "1"); (c) ω = 3.15, (n/m, j) = (1/3, 1)

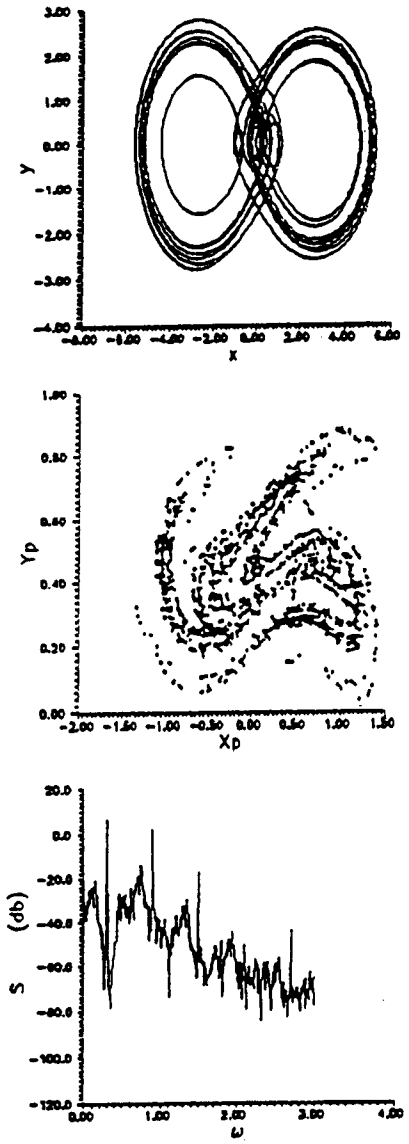

FIG. 7. Chaotic Attractor in Ultrasubharmonic Domain [ω = 0.33, (n/m, j) = (7/3, ∞)]

furcation (see Fig. 10, Gottlieb and Yim 1992) governed by (7*b*) [shown here in Fig. 2(a)] is described by the ordering index in the subharmonic domain j: 1, 2 for n/m = 1/2 (e.g., $R_{1/2,1} \rightarrow R_{1/2,2}$). Note that period doubling in the ultraharmonic domain (see Fig. 11, Gottlieb and Yim 1992) is described by j: 2, 3 for n/m = 2/1 (e.g., $R_{2/1,2} \rightarrow R_{2/1,3}$).

Numerical simulations of system response enable construction of a schematic bifurcation diagram (Fig. 4). The simulations consist of changing one control (ω) for a given parameter space under various sets of initial conditions. The diagram depicts existence of periodic orbits throughout the domain described by a variety of subharmonic and ultrasubharmonic solutions. Solutions are separated by a common periodicity index m. Symmetric (S) and asymmetric (AS) solutions ($n/m = n/1$) describing pitchfork bifurcation transitions are also depicted. For convenience, resonance lines ($R_{n/m}$ in dashed lines) are added to highlight solution ordering. An example is the $R_{7/3,1}$ ultrasubharmonic response (Fig. 4: $\omega \simeq 4$, n/m = 7/3) found between the resonance lines of $R_{3/1}$ and $R_{2/1}$. While not all of the ultrasubharmonics predicted by the resonance number ordering are numerically identified, the dominant harmonic and lower order subharmonic and ultrasubharmonic solutions are found to be accurately described. Note that in order to obtain the complete nonlinear steady state responses, fractal basin boundaries describing all possible initial conditions need to be considered.

ROUTES TO CHAOTIC RESPONSE

Possible routes to a strange attractor can be described by the evolution of unsymmetric and symmetric solutions as is evident by the spectral content of the prechaotic and postchaotic motions. One possible route is through smooth and continuous period multiplying. This route includes period doubling (Fig. 5) and can be traced in the superstructure by the ordering index j: 2, 4, 8$\cdots$ (e.g., $R_{1/2,1} \rightarrow R_{1/2,2} \rightarrow R_{1/2,4} \rightarrow R_{1/2,8}$). The period doubling route to chaotic motion is observed with the appearance of additional even (Fig. 5) harmonics. Similarly, a period tripling route with the appearance of additional odd harmonics j: 3, 9 (e.g., $R_{1/3,1} \rightarrow R_{1/3,3}\cdots$) (not shown here due to space limitation) has been identified and verified numerically. Thus, the period multipling scenario describes an accumulation of internal resonance horns in the bifurcation sets. Note that when the multiplying sequence is infinite, the dimension index [d], describing the number of systems degrees of freedom, does not retain its integer value and is replaced by a characteristic fractal dimension [e.g., $R_{\text{"1/2",}\infty,\text{"2.31"}}$ in Fig. 5(c)].

Based on our detailed numerical study, another route to chaotic motion is found in the abrupt change to and from neighboring periodic motions (e.g., $R_{1/1,1} \rightarrow R_{1/3,1}$, as shown in Fig. 6). This occurs near the local tangent bifurcation values and is associated with contraction of the $2m\pi/n$ ultrasubharmonic. This route is found to be short lived in parameter space and culminates in a strange attractor when a "collision" occurs between two neighboring attractors separated by a saddle (i.e., bifurcation defined as a heteroclinic tangency). For the moored ocean system strange attractors are found for odd (m and n odd) self-similar subharmonic (e.g., $R_{\text{"1/3",}\infty,\text{"2.57"}}$, Fig. 6) and ultrasubharmonic (e.g., $R_{\text{"7/3",1,"2.63"}}$, Fig. 7) scenarios while even (m or n even) ultrasubharmonic scenarios of unsymmetric solutions are portrayed only by transient chaotic behavior.

CONCLUDING REMARKS

A less recognized but important (and potentially beneficial) aspect of highly nonlinear global response behavior, namely the underlying universal pattern, of a system with complex nonlinearities is examined here in detail. Specifically, the intricate superstructure in bifurcation sets and possible routes to chaotic response of a multipointed, submerged, moored, ocean system with complex nonlinearities in the stiffness and exciting forces subjected to monochromatic waves is investigated analytically and demonstrated numerically. Bifurcations are identified in parameter space by employing a local stability analysis, and the steady-state superstructure in the bifurcation sets is further revealed by extensive numerical simulations.

A resonance number consisting of suffices describing the nonlinear content and dimension of solution within the bifurcation structure is derived. Resonance number ordering reveals the structure near resonances and enables the prediction of occurrence of highly nonlinear responses, e.g., subharmonics, ultraharmonics, ultrasubharmonics, and chaos. The resulting superstructure identifies the mechanisms governing system stability and the onset of strange attractors. In addition to a smooth transition of infinite sequence of period multiplying (e.g., doubling and tripling) to chaos, another possible route to chaos via sudden explosion (collision of nearby attractors separated by a saddle) is also observed and numerically demonstrated.

ACKNOWLEDGMENT

The writers gratefully acknowledge the financial support from the United States Office of Naval Research, Grant No. N00014-92-1221.

APPENDIX I.

$$R = \alpha \left\{ x - \tau \left[\frac{\beta + x}{\sqrt{1 + (\beta + x)^2}} - \frac{\beta - x}{\sqrt{1 + (\beta - x)^2}} \right] \right\}$$

$$F_D = \mu\delta \left(u - \frac{y}{\omega} \right) \left| u - \frac{y}{\omega} \right|; \quad F_I = \mu\omega^2 \left[\frac{\partial u}{\partial \theta} + \left(u - \frac{y}{\omega} \right) \frac{\partial u}{\partial x} \right]$$

$$u = f_0 + f_1 \cos(\kappa x - \theta)$$

$$\alpha = \frac{4K}{M + \rho \forall C_A}; \quad \beta = \frac{2b - L}{2d}; \quad \tau = \frac{l_c}{2d}; \quad \gamma = \frac{C}{M + \rho \forall C_A}$$

$$\delta = \frac{1}{2} \frac{C_D}{1 + C_A} \frac{A_P}{\forall} g\kappa \tanh(\kappa h'); \quad \mu = \frac{\rho \forall (1 + C_A)}{M + \rho \forall C_A}$$

$$f_0 = \frac{U_0}{\omega d}; \quad \chi = ka; \quad \kappa = kd; \quad h' = \frac{h}{d}; \quad f_1 = \frac{\chi}{\kappa} \frac{\cosh(\kappa h')}{\sinh(\kappa h')}$$

APPENDIX II. REFERENCES

Arnold, V. I. (1965). "Small denominators: I. mapping of the circumference onto itself." *Am. Math. Soc. Transl. Ser.*, 2, 46, 213–284.

Bernitsas, M. M., and Chung, J. S. (1990). "Nonlinear stability and simulation of two-line ship towing and mooring." *Appl. Oc. Res.*, 11, 153–166.

Devaney, R. L. (1986). *An introduction to chaotic dynamical systems.* Benjamin-Cummings Publication Co., Redwood City, Calif.

Feder, J. (1989). *Fractals.* Plenum Publishing Corp., New York, N.Y.

Feigenbaum, M. J. (1980). "Universal behavior in nonlinear systems." *Los Alamos Sci.*, 1, 4–27.

Gottlieb, O., and Yim, S. C. S. (1992). "Nonlinear oscillations, bifurcations and chaos in a multi-point mooring system with a geometric nonlinearity." *Appl. Oc. Res.*, 14, 241–257.

Grebogi, C., Ott, E., and York, J. A. (1983). "Crises, sudden changes in chaotic attractors and transient chaos." *Physica D*, 7, 181–200.

Grebogi, C., Ott, E., and York, J. A. (1987). "Basin boundaries metamorphoses: changes in accessible boundary orbits." *Physica D*, 24, 243–262.

Guckenheimer, J., and Holmes, P. (1986). *Nonlinear oscillations, dynamical systems and bifurcation of vector fields.* Springer-Verlag New York, New York, N.Y.

Holmes, P., and Whitley, D. (1984). "Bifurcations of one and two dimensional maps." *Philosophical Trans. Royal Soc.*, London, U.K., A, 311, 43–102.

Ioos, G., and Joseph, D. D. (1981). *Elementary stability and bifurcation theory.* Springer-Verlag New York, New York, N.Y.

Jensen, M. H., Kadanoff, L. P., Libchaber, A., Procaccia, I., and Savans, J. (1985). "Global universality at the onset of chaos: results of a forced Rayleigh-Bénard experiment." *Phys. Rev. Lett.*, 55, 2798–2801.

Parlitz, U., and Lauterborn, W. (1985). "Superstructure in the bifurcation set of the Duffing equation." *Phys. Lett.*, A, 107, 8, 351–355.

Simoyi, R. H., Wolf, A., and Swinney, H. L. (1982). "One dimensional dynamics in a multicomponent chemical reaction." *Phys. Rev. Lett.*, 49, 245–248.

Thompson, J. M. T., and Soliman, M. S. (1990). "Fractal control boundaries of driven oscillators and their relevance to safe engineering design." *Proc., Royal Soc. London*, London, U.K., A, 428, 4–13.

Thompson, J. M. T., and Stewart, H. B. (1986). *Nonlinear dynamics and chaos.* Wiley, Chicester.

Triantafyllou, M. S., and Yue, D. K. P. (1995). "Damping amplification in highly extensible hysteretic cables." *J. Sound and Vibration*, 186, 355–368.

Ueda, Y. (1980). "Steady motions exhibited by Duffing's equation: a picture book of regular and chaotic motions." *New approaches to nonlinear problems in dynamics*, P. Holmes, ed., 311–322.

Ueda, Y. (1981). "Explosions of strange attractors exhibited by Duffing's equation." *Annu. N.Y. Acad. Sci.*, 357, 422–434.

Ueda, Y., Yoshida, S., Stewart, H. B., and Thompson, J. M. T. (1990). "Basin explosions and escape phenomena in the twin-well Duffing oscillator: compound global bifurcations organizing behavior." *Philosophical Trans. Royal Soc. Lond.*, London, U.K., A, 332, 169–186.